Available online at www.sciencedirect.com
SCIENCE DIRECT®
Journal of Membrane Science 236 (2004) 101–108
journal of MEMBRANE SCIENCE
www.elsevier.com/locate/memsci

Gas transport efficiency of ceramic membranes: comparison of different geometries

Tijana Zivkovic [a,1], Nieck E. Benes [b], Henny J.M. Bouwmeester [a,*]

[a] *Inorganic Materials Science, Faculty of Science and Techology & MESA, Institute for Nanotechnology, University of Twente, P.O. Box 217, 7500 AE Enschede, The Netherlands*
[b] *Process Development Group, Technical University of Eindhoven, P.O. Box 513, 5600 MB Eindhoven, The Netherlands*

Received 24 November 2003; received in revised form 20 February 2004; accepted 20 February 2004

Abstract

The effect of support geometry on the performance of asymmetric ceramic membranes for gas separation is analyzed. Flat plate (FP), tubular (TU) and multichannel (MC) geometries are investigated using the dusty gas model (DGM) to describe transport of a multicomponent gas mixture through the macroporous support. It is shown that: (a) the support geometry significantly affects membrane performance; (b) in the case of the multichannel geometry, the inner channels do not contribute efficiently to the overall gas transport; (c) best performance in terms of both flux and permselectivity is obtained for tubular geometry. It is furthermore clarified that for an accurate description of the transport behaviour it is crucial to properly account for the relative contributions of all different transport mechanisms (Knudsen diffusion, bulk diffusion and viscous flow) included in the DGM.

Keywords: Support resistance; Multichannel; Gas transport; Ceramic membranes; Dusty gas model

1. Introduction

In the petrochemical industry, energy and equipment savings can be obtained if selective membrane separation of hydrogen from a gas mixture is employed in processes such as steam reforming, water–gas shift reaction, hydrocarbons dehydrogenation [1,2]. To ensure high separation and permeation rates, while still retaining mechanical stability in harsh application conditions (chemically aggressive environment and high temperature), asymmetric ceramic membranes are usually employed. An ultrathin separation layer is superimposed onto one or more intermediate layers that, in turn, are supported on a mechanically strong base support. This results in a graded pore structure across the membrane. Large dimensions (thickness) of the base support, compared to those of the selective layer, may induce a high resistance to mass transport that can even be dominant for the highly permeable gases (H_2,He) [3] (although for most of the gases the top selective layer determines transport).

Membrane systems consist of membranes elements or modules. They often involve a tubular (TU) geometry rather than flat plate (FP). Though multichannel (MC) monolithic elements provide a greater surface-area-to-volume ratio and mechanical robustness, the use of multitubular modules allows for easy change of faulty elements. The packing density can be further increased by the use of hollow fiber geometry with even smaller overall membrane thickness and, hence, reduced support resistance [1].

The aim of this paper is to investigate the influence of support geometry on the overall membrane performance of asymmetric ceramic membranes for gas separation. Due to the complex set of interrelated parameters, numerical simulations are usually employed for this kind of analysis. In the field of gas separation such studies are scarce. For micro- and ultra-filtration membranes, Dolecek and Cakl [4] have shown that increasing the packing density does not generally lead to enhanced membrane performance. The authors showed, experimentally and theoretically, that channel contributions to the total permeate flux through a 19-channel

* Corresponding author. Tel.: +31-53-489-2202.
E-mail addresses: h.j.m.bouwmeester@tnw.utwente.nl (H.J.M. Bouwmeester), t.zivkovic@ct.utwente.nl (T. Zivkovic).
[1] Tel.: +31-53-489-2993; fax: +31-53-489-4683.

0376-7388/$ – see front matter © 2004 Elsevier B.V. All rights reserved.
doi:10.1016/j.memsci.2004.02.011

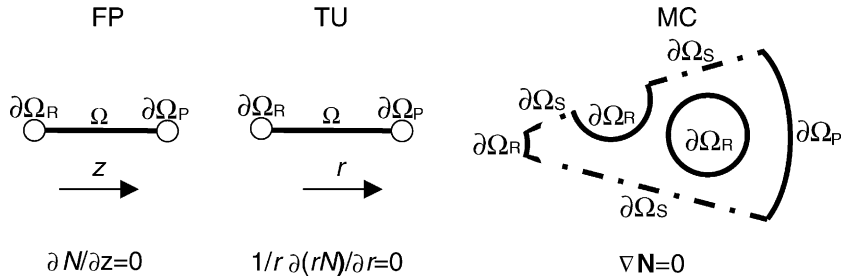

Fig. 1. Calculation domains Ω with boundaries $\partial\Omega$ and flux expressions for the three support geometries: FP, TU and MC.

hexagonal ceramic membrane depend on the ratio of the selective-layer to porous-support permeabilities. However, these parameters vary with membrane geometry and the type of application. In this paper, we address this issue for gas separation considering different membrane geometries. To the best of our knowledge, it is the first time that the effect of support geometry on the transport of a multicomponent gas mixture through asymmetric ceramic membranes is considered, in terms of both flux and selectivity.

1.1. Base cases

To enable comparison of the effect of support geometry on overall membrane performance, the following support geometries are considered:

1. Flat plate (FP).
2. Tubular (TU).
3. Multichannel (MC).

The corresponding calculation domains Ω and boundary condition lines $\partial\Omega$ (Fig. 1) are determined by transport direction and symmetry considerations, which are addressed later in more detail. The macroscopic dimensions of the support geometries match those of commercially available ceramic membrane supports. Parameters used in calculation for both top layer and membrane support, are listed in Table 1.

For a single-species gas, hydrogen, and in the case of a binary gas mixture hydrogen and methane are considered as the permeating gases. The flux through the selective layer is assumed to be linearly dependent on the partial pressure difference across the layer, with the permeability F_i (mol m^{-2} s^{-1} Pa^{-1}) of gas species i as the parameter of proportionality. This would, for instance, correspond to transport through a microporous silica layer at high temperature, i.e. in the Henry regime. The permeability of silica for hydrogen is varied over a very wide range of values, from 10^{-20} to 1 mol m^{-2} s^{-1} Pa^{-1}, which includes the value $\sim 10^{-6}$ mol m^{-2} s^{-1} Pa^{-1} observed for state-of-the-art silica membranes [5]. Since our interest involves the hydrogen permeability, this quantity is referred to as F in the remainder of the text. Different values for the pressure difference are considered (Table 1). Each of these values corresponds to different contributions of the involved transport mechanisms, i.e. Knudsen diffusion, viscous flow and bulk diffusion.

2. Theory

For an isothermal system at steady-state, in the absence of chemical reactions, conservation of mass requires that the divergence of the flux $\boldsymbol{N}_i$ (mol m^{-2} s^{-1}) of a gaseous component i vanishes

$$\nabla \cdot \boldsymbol{N}_i = 0 \tag{1}$$

where ∇ is the differential operator $(\partial/\partial x, \partial/\partial y, \partial/\partial z)$, with spatial coordinates x, y, and z. Transport in a flat plate geometry occurs in one direction and, consequently, for its description only a single coordinate is required. Transformation to polar coordinates and taking advantage of the axial symmetry also renders transport in the tubular geometry into a one-dimensional (1D) problem. For the multichannel geometry two independent coordinates (x, y) remain and, due to symmetry considerations, the calculation domain only covers 1/12th of the actual 19-channel MC membrane cross-section. Fig. 1 depicts the corresponding calculation domains Ω and boundary conditions $\partial\Omega$.

Table 1
Properties of the top layer and membrane support, and the investigated process parameters

Material properties		Process parameters			
Top layer (SiO_2)	Support layer (Al_2O_3)	Pressure (bar)			T (K)
		Case	p^{ret}	p^{perm}	
F (mol m^{-2} s^{-1} Pa^{-1}) $= 10^{-20}$–1	ε (–) $= 0.3$, τ (–) $= 3$, d_p (m) $= 7 \times 10^{-6}$	A	2	10^{-4}	873
		B	32	30	
		C	30	1	

In the solution domain Ω, three different categories of boundaries $\partial\Omega$ can be distinguished:

1. $\partial\Omega_S$: symmetry, $-\boldsymbol{n}\cdot\boldsymbol{N}_i = 0$;
2. $\partial\Omega_P$: permeate side, fixed pressure, $p_i = p_i^{\text{perm}}$;
3. $\partial\Omega_R$: retentate side, flux through selective layer, $-\boldsymbol{n}\cdot\boldsymbol{N}_i = F_i(p_i^{\text{ret}} - p_i)$.

where $\boldsymbol{n}$ is the outward normal vector on $\partial\Omega$. The partial pressures p_i (Pa) at both permeate and retentate side are assumed constant.

2.1. Flux expressions

Transport of gas mixtures in porous media has been studied extensively, and abundant theoretical descriptions have been proposed in the open literature. Present and DeBethune [6] presented flux expressions for the transport of a binary mixture in a long capillary, based on a momentum approach. They assumed that diffusive and viscous transport are simply additive and obtained expressions that are essentially the same as those provided by the well-known dusty gas model (DGM) (e.g. [7]) for transport of gas mixtures in porous media. For most practical problems, these expressions are generally considered adequate.

2.1.1. Binary system

For a binary mixture, the flux ($\boldsymbol{N}_i$) expressions can be written as

$$RT\,\boldsymbol{N}_i = -\frac{\mathcal{D}_{ij}^0}{\mathcal{D}_{ij}^0 + p_i D_j + p_j D_i} D_i \nabla p_i - \left(\frac{B_0}{\eta} + \frac{D_i D_j}{\mathcal{D}_{ij}^0 + p_i D_j + p_j D_i}\right) p_i \nabla(p_i + p_j) \quad (2)$$

where the interchangeable indices i and j refer to either H_2 or CH_4, R and T have their usual meaning and η is the viscosity (Pa s). B_0 is a parameter related to the structure of the porous medium (m^2) and can be obtained from experiment or, assuming cylindrical pores, estimated from [7]

$$B_0 = \frac{\varepsilon d_p^2}{32\tau} \quad (3)$$

with ε (–) the porosity, τ (–) the tortuosity and d_p (m) the pore diameter.

Expression (2) contains three different diffusion coefficients, two of which (D_i and D_j ($m^2\,s^{-1}$)), are related to diffusion in the free molecule or Knudsen regime. These diffusion coefficients depend on the molar mass M_i ($g\,mol^{-1}$) of the gaseous species and on temperature via

$$D_i = \frac{4}{3} K_0 \sqrt{\frac{8RT}{\pi M_i}} \quad (4)$$

where K_0 is a parameter related to the structure of the porous medium (m). Assuming cylindrical pores K_0 can be estimated from [7]

$$K_0 = \frac{\varepsilon d_p}{4\tau} \quad (5)$$

The other diffusion coefficient $\mathcal{D}_{ij}{}^0$ accounts for binary collisions between the two gaseous species. It is related to the binary diffusion coefficient D_{ij} by

$$\mathcal{D}_{ij}^0 \equiv p\frac{\varepsilon}{\tau} D_{ij} \quad (6)$$

where multiplying with ε over τ is performed to account for the structure of the porous medium. For non-polar gases, the binary diffusion coefficient can be estimated from the expression given by Fuller et al. [8]

$$D_{ij} = 1.013 \times 10^{-2} \frac{T^{1.75}}{p(v_i^{1/3} + v_j^{1/3})^2} \sqrt{\frac{M_i + M_j}{M_i M_j}} \quad (7)$$

where v (m^3) is the diffusion volume of a species and M_i ($kg\,mol^{-1}$) is the molar mass. Employing expression (7) the multiplication with the total pressure renders $\mathcal{D}_{ij}^0$ to be independent of pressure.

2.1.2. Unary system

For single component gas transport, DGM Eq. (2) reduces to the following flux expression:

$$\boldsymbol{N}_i = -\frac{1}{RT}\left(D_i + \frac{B_0}{\eta} p\right) \nabla p \quad (8)$$

The first and second term on the right hand side account for the diffusive and convective contribution to the total flux, respectively.

2.2. Comparison

A comparison between the geometries in terms of membrane performance is made on the basis of pure H_2 flux and H_2/CH_4 selectivity for a 50–50% binary mixture. The pure hydrogen flux is normalized with respect to the surface area of the silica layer on the retentate boundary $\partial\Omega_R$

$$< N >= \frac{\int_{\partial\Omega_R} -\boldsymbol{n}\cdot\boldsymbol{N}\, d(\partial\Omega)}{\int_{\partial\Omega_R} d(\partial\Omega)} \quad (9)$$

In case of MC geometry, we can distinguish three boundaries on the retentate side, each corresponding to a channel l. The channel efficiency is defined as

$$\xi_l \equiv \frac{< N_l >}{< N_{\text{tot}} >} \quad (10)$$

where the total flux $< N_{\text{tot}} >= \sum < N_l >$ is the sum of the normalized fluxes of all three channels.

2.3. Numerical solution

Numerical simulations were performed using the FEMLAB® software package. Files used for the calculations can be found at the Internet site: http://www.ims.tnw.utwente.nl/.

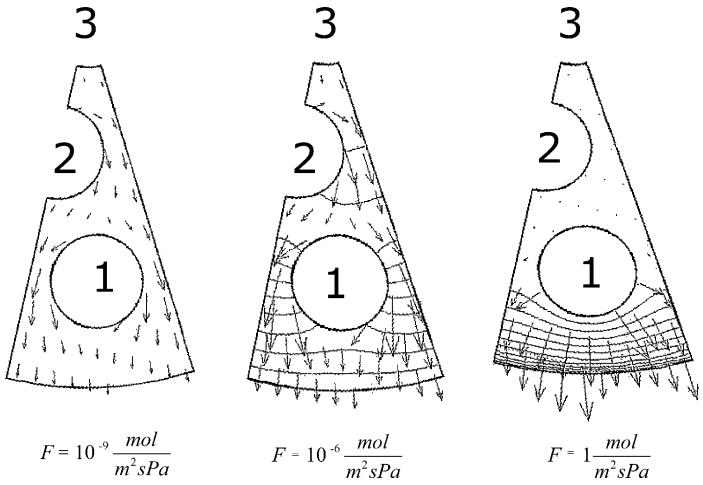

Fig. 2. 2D-pressure profiles (isobars) and 2D flux profiles (arrows) as a function of permeability of silica in MC membranes for unary system for pressure case C. Very low F (a), value for the state-of-the-art (b) and very high F (c).

3. Results

3.1. Unary system

From a practical point of view, the tubular and multichannel geometries are considered to be the most suitable due to their greater surface-area-to-volume ratio and mechanical robustness. Consequently, emphasis will be on the comparison of these two geometries. Calculations showed that the same general trend holds for all pressure differences, which is why only case C is discussed in more detail below.

The pressure and flow profiles over a solution domain (1/12 of multichannel cross-section) are presented in Fig. 2 for permeation of pure hydrogen in case of a high trans-membrane pressure difference (case C) for three distinctive values of the permeability of silica, i.e. F being very low, state-of-the-art or very high. Very low values of F (Fig. 2a) correspond to almost impermeable dense silica layers. In this case, the major part of the transport resistance and, hence, gradients in pressure are located in these thin layers. The pressure in the supporting structure is more or less constant and equal to p^{perm}. The fluxes in the support are low and gradually increase in the direction towards the outside of the MC membrane.

In the extreme case of a very high permeability of silica (Fig. 2c), the thin silica layers pose nearly no resistance. Hence, transport behavior in this case is entirely determined by the support. Here, the MC geometry induces a distinctive pressure profile, i.e. the pressure gradient is entirely located on the outside of the MC membrane. Consequently, only a small portion of each outer channel contributes to the total flux, while the central portion of the entire multichannel element shows negligible contribution.

Fig. 2b corresponds to an intermediate situation, in which the pressure changes are located within the silica layers as well as in the entire support. In this case all channels contribute to the total flux, albeit that the outer channels contribute more.

Fig. 3 shows the channel efficiency (Eq. (10)) for each channel as a function of the permeability of silica. For low values of the permeability, the influence of the support is negligible (analogous to Fig. 2a) and the efficiency of each channel is the same (1/3). Around the state-of-the-art value, the inner channels show a distinct decrease in efficiency with increasing permeability of silica, accompanied by an increase in the efficiency of the outer channels. For high permeability of the silica layer, only the outer channel contributes to the flux.

The reduced efficiency of the inner channels of a MC membrane suggests that the performance of a thin silica layer

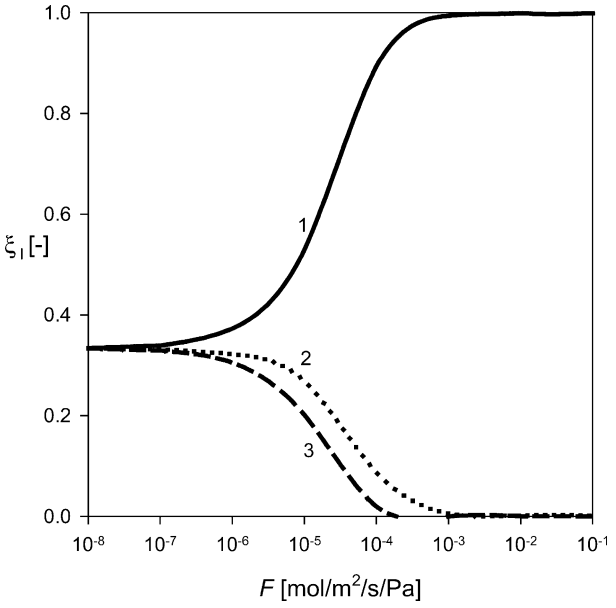

Fig. 3. Channel efficiency (Eq. (10)) in MC membranes for unary system and pressure case C. Labels correspond to the different channels as in Fig. 2.

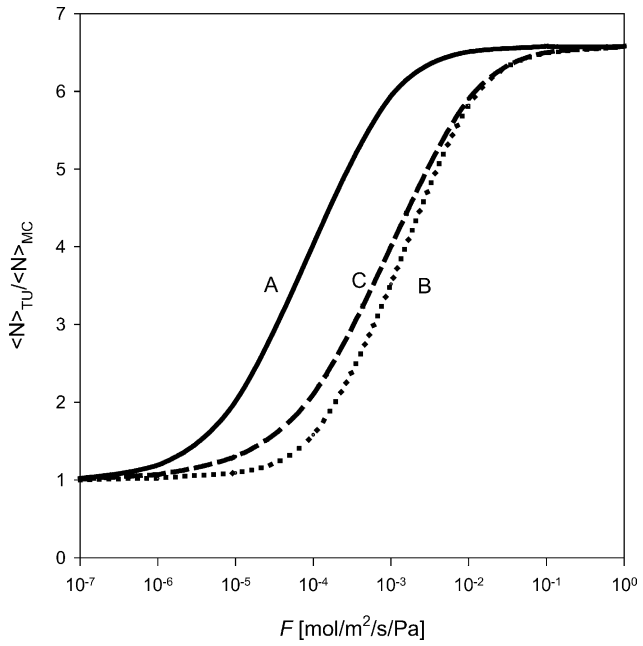

Fig. 4. Flux normalized with respect to the surface area of silica for TU and MC membranes as a function of permeability of silica, for unary system and pressure cases A, B, and C.

will be better when applied onto tubular support geometry. Fig. 4 shows the ratio of fluxes, normalized with respect to the total surface area of silica, for both tubular and multichannel membranes as a function of the permeability of silica. It can be seen that the flux per surface area of silica is distinctly higher for tubular membranes for all three considered cases of the pressure difference. For low permeability F the resistance imposed by the silica layer is dominant and the normalized flux is independent of the properties of the support, causing $< N_{TU} > / < N_{MC} >$ to be close to unity.

When the permeability F of silica increases, the influence of the support becomes more significant. The reduced efficiency of the inner channels causes a reduced performance of the MC membranes compared to the TU membranes. Clearly, the change in $< N_{TU} > / < N_{MC} >$ with F is different for the various cases of pressure difference. For the low pressure difference case (case A) the reduced performance of the MC membranes occurs at lower F value. This is due to the high support resistance in case A (i.e. due to a smaller viscous flow term). For the high pressure difference case (case C), the viscous flow term is larger and the resistance of the support is much lower compared to the low pressure difference case. Consequently, a much higher permeability of silica is allowed before the support resistance becomes significant. It should be noted that even for the low pressure difference case (case A), the Knudsen number (ratio of the mean free path λ of the molecules and the pore radius d_p) is smaller than 0.01, indicating that the Knudsen diffusion contribution is negligible compared to viscous transport. When a support with much smaller pores would be used, the Knudsen contribution might have been the governing transport mechanism, and the lines in Fig. 4 would have shifted much more to the left.

For highly permeable silica, overall transport is governed by the support. Surprisingly, the ratio $< N_{TU} > / < N_{MC} >$ reaches an asymptotic value (6.58), which is identical for all three cases of the pressure difference. The asymptotic value is not related to the pressure or temperature, but only arises from differences in geometry. For a comparison between MC and TU membranes, sophisticated numerical methods are required, such as the finite element method employed here. However, for a comparison between TU and FP geometry in this asymptotic regime an analytical solution can be found for the flux

$$N_{FP} = -\frac{1}{RT\delta}\left(D + \frac{B_0}{\eta}p_{av}\right)\Delta p$$
$$N_{TU} = G \times N_{FP} \tag{11}$$

where p_{av} is the average of the permeate and retentate pressures. The geometrical factor G expresses the influence of the curvature on the support resistance

$$G = \frac{a}{\pm\ln(1 \pm a)} \tag{12}$$

where $a = \delta/r$ is the ratio of the support thickness δ and the inner radius r. The positive signs are valid in case the silica layer is on the inside of the tube. Then, for all a, G exceeds unity, signifying that the flux through a tubular membrane is always larger than through a flat membrane of the same thickness. For $r \gg \delta$, $G \rightarrow 1$, i.e. the effect of curvature disappears. When it is assumed that the silica layer is on the outside of the tube (corresponding to negative signs in Eq. (12)), the flux with respect to the outside of the tube is relevant and curvature has a negative effect on the flux.

The surface area of silica is generally larger in a multichannel membrane than in a tubular membrane of the same length. To account for this, we calculated the number of required tubes to obtain the same performance as one multichannel element. The result is depicted in Fig. 5 as a function of permeability F of silica. For all three cases of the investigated trans-membrane pressure difference, the number of required tubes decreases as the performance of silica improves, especially for state-of-the-art values of F. For the chosen commercial multichannel element and tubular membranes, the ratio A of the silica surface areas of multichannel and tubular supports is 10.85. In the case of almost impermeable silica A equals the number of tubes required to achieve the same performance as an MC membrane. As the permeability of silica increases, the number of required tubes decreases dramatically and finally reaches the asymptotic value of 1.67 (= A/G).

3.2. Binary system, MC geometry

The performance of a membrane is not merely determined by the flux of the desired species, but also by the selectivity towards this species. In the remainder it is assumed that the

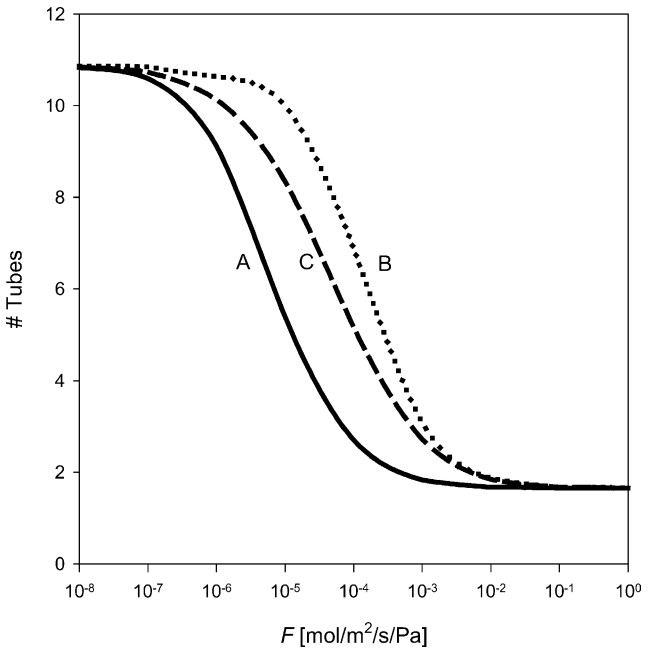

Fig. 5. The number of tubes, required to acquire the same performance as one multichannel element, as a function of permeability of silica for unary system for pressure cases A–C.

intrinsic selectivity (i.e. the permselectivity of only the thin silica layer) for H_2 over CH_4 is 500 [5]. Due to the presence of the support the actual selectivity will be less than 500. In Fig. 6, the selectivity F_α for the different channels in an MC membrane is plotted as a function of the hydrogen permeability F of silica for the pressure difference of case C. Clearly, the increase in F corresponds to a rise in the contribution of the support resistance, resulting in a decline of the selectivity. The decline in selectivity is most remarkable for the inner channels, for which even selectivities below unity are observed. This corresponds to a higher transport rate of CH_4 compared to H_2, suggesting that plugging of the inner channels would improve the performance. The reversed selectivity can be explained as follows. At high F_i values, the MC membrane will fill up with hydrogen, causing a decline in the flux of this gas in the inner channels. The permeance of CH_4 through the silica is much lower and the effect of filling up is less pronounced. Consequently, a smaller decline in CH_4 flux is expected.

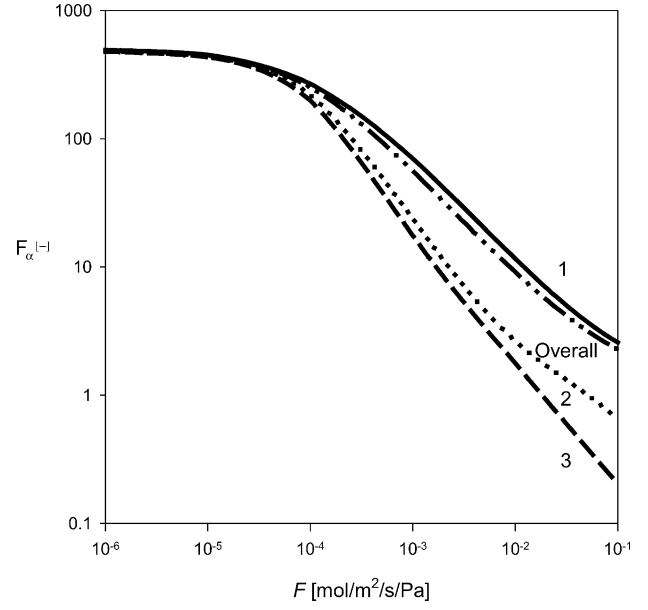

Fig. 6. Permselectivity per channel in MC membranes in case of no defects in silica layer for the pressure case C. Labels correspond to the different channels as indicated in Fig. 2.

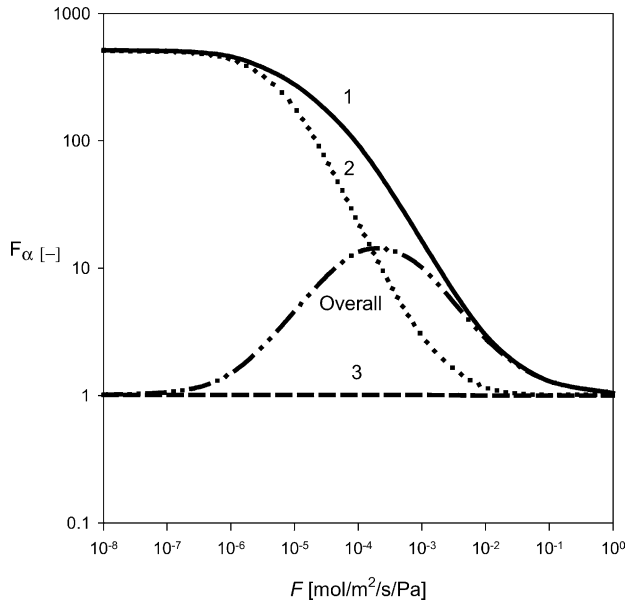

Fig. 7. Permselectivity per channel (labeled as in Fig. 2) in MC membranes in case of defects in silica layer for the low pressure case (case A).

In Fig. 7, the selectivity is depicted for an MC membrane with a defective silica layer on the inside of channel 3, calculated for the low pressure difference (case A). Clearly, for low F-values, the overall transport is largely determined by the defective channel. Almost all gas permeates from channel 3 to the outside of the MC membrane, while the contribution of the other channels to the flow is negligible. As can be expected from the small value (<0.01) of the Knudsen number Kn (ratio of the mean free path λ of the molecules and the pore radius d_p), the transport is dominated by the pressure-dependent second term in Eq. (2) and, hence, selectivity is low.

With an increase in F the contributions of channel 2 and in particular that of channel 1 become more important and the overall selectivity increases. Concurrently, the influence of support resistance becomes larger with F. This leads to a decrease in the apparent selectivity of channels 1 and 2 similar to that observed in Fig. 6. At a certain F, the increase in the contribution of both channels to the total flow and the decrease in their apparent selectivity cancel each other out exactly. At this point, the selectivity of the MC membrane reaches a maximum value of approximately 10, which

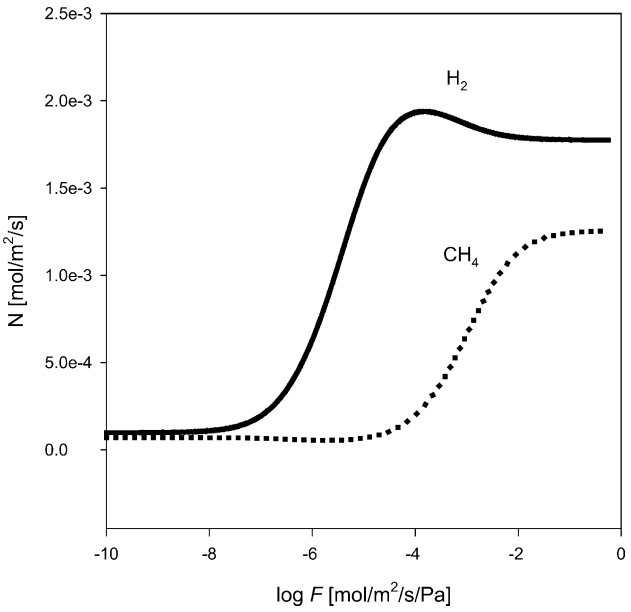

Fig. 8. Flux of hydrogen and methane in MC membranes with defective silica layer on the inside of channel 3 as a function of permeability of silica for the low pressure case (A) and smaller pore size of the support material $d_p^{sup} = 0.7\,\mu m$.

is small compared to the intrinsic selectivity of 500. Further increase of F leads to a more dominating support resistance, and consequently a decrease in the selectivity of the MC membrane. The position of the maximum is obviously dependent on the relative resistance of the support. For instance, the maximum shifts to the left upon decreasing pore size of the support material.

The fluxes of hydrogen and methane corresponding to Fig. 7 are predominantly governed by viscous transport and, consequently, show a monotonic increase with F. The maximum in overall selectivity is due to a change in the relative transport contributions of the silica layer and the support. When the pore size of the support is decreased, the viscous contribution is lowered compared to the diffusive contribution and the maximum in selectivity shifts towards lower F. In Fig. 8, the fluxes of hydrogen and methane are depicted for the case $d_p = 7 \times 10^{-7}$ m, and again a defective silica layer on the inside of channel 3. Remarkably, for this case the hydrogen flux shows a maximum at a certain value of F. This indicates that improvement of the permeability of the silica membrane layer beyond a certain value would even result in decreased performance of the multichannel membrane.

The increased number of intermolecular collisions with increasing methane concentration can explain the decrease in hydrogen flux observed for high permeability of silica. During these collisions, momentum is transferred from the fast moving hydrogen to the less mobile methane, moderating the hydrogen flux while increasing the methane flux. It should be noted that there is still an overall selectivity at infinite value of F. This can only be attributed to the difference in mass of the permeating gases, i.e. the Knudsen diffusion contribution. Consequently, for a prediction of transport behaviour, it is crucial to properly account for the three transport mechanisms included in the DGM.

4. Summary and conclusions

The effect of support geometry on multicomponent gas transport through microporous silica composite membranes was investigated under several trans-membrane pressure differences. Multichannel, tubular and flat plate geometries were compared on the basis of pure H_2 flux and H_2/CH_4 selectivity for a 50–50% binary mixture. The dusty gas model was used to account for the properties of the multicomponent gas mixture, membrane matrix and the governing transport mechanisms. Numerical simulations were performed using the FEMLAB® software package.

It is shown that the MC support geometry imposes a severe resistance to gas transport, inducing a distinct pressure profile. For highly permeable silica, the transport is entirely dominated by the support, i.e. the pressure gradients are entirely located on the outside of the MC membrane. Hence, only a small portion of the outer channels contributes to the total flux, while the central portion of the multichannel module shows negligible fluxes. This suggests that the performance of the thin silica layer will be improved when applied onto a tubular support. Indeed, for all investigated pressure differences the flux per surface area silica for this geometry is clearly higher than for a multichannel geometry. The $< N_{TU} > / < N_{MC} >$ flux ratio reaches an asymptotic value (6.58), which is identical for all considered pressure differences. This indicates that the asymptotic value is neither related to pressure nor temperature, but arises only from differences in the geometry. Consequently, as the performance of silica improves, the number of required tubes to obtain the same performance as the MC membrane decreases dramatically to the value of 1.67. Hence, the high packing densities, i.e. high surface area to volume ratio, for multitubular and multichannel membrane modules only translate into optimum performance for the former case.

In terms of permselectivity, the inner channels also show a considerable decline, and even selectivities below unity are observed (Fig. 6). This corresponds to a higher transport rate of CH_4 compared to H_2, suggesting that plugging, i.e. exclusion, of the inner channels would improve the performance. When the inner channel is leaking, a maximum in selectivity is observed for a certain value of F. Due to intermolecular collisions, the flux of hydrogen may also show a maximum with F, suggesting that further improvement of the silica layer would result in a decreased performance of the MC membrane.

Finally, the present study demonstrates that for accurate description of the gas transport it is crucial to properly account for the relative contributions of Knudsen diffusion, bulk diffusion and viscous flow, which are included in the DGM.

Acknowledgements

Financial support of EU project CERHYSEP number GRD1-2001-40315 is gratefully acknowledged.

Nomenclature

a	ratio of the support thickness and the inner radius of a tubular membrane (–)
A	ratio of silica surface areas of multichannel and tubular supports (–)
B_0	structure parameter of the porous medium (m^2)
d_p	pore diameter (m)
D_i	diffusion coefficient of gaseous species i in the free molecule, or Knudsen regime ($m^2\,s^{-1}$)
D_{ij}	binary diffusion coefficient ($m^2\,s^{-1}$)
$Đ_{ij}{}^0$	diffusion coefficient that accounts for binary collisions between the two gaseous species i, j ($m^2\,s^{-1}$)
F	permselectivity (–)
F_i	permeability of gaseous species i ($mol\,m^{-2}\,s^{-1}\,Pa^{-1}$)
G	ratio of fluxes through tubular and multichannel membrane, which are normalized with respect to the surface area of the silica layer (–)
Kn	Knudsen number (–)
K_0	structure parameter of the porous medium (m)
M_i	molar mass of gaseous species i ($g\,mol^{-1}$)
N_i	flux of gaseous species i ($mol\,m^{-2}\,s^{-1}$)
$< N_l >$	flux through channel l normalized with respect to the surface area of the silica layer on the retentate boundary ($mol\,s^{-1}$)
$< N_{MC} >$	flux through multichannel membrane normalized with respect to the surface area of the silica layer ($mol\,s^{-1}$)
$< N_{tot} >$	total flux as sum of the normalized fluxes of all three channels ($mol\,s^{-1}$)
$< N_{TU} >$	flux through tubular membrane normalized with respect to the surface area of the silica layer ($mol\,s^{-1}$)
p_{av}	average of the permeate and retentate pressures (Pa)
p_i	partial pressure of gaseous species i (Pa)
p_i^{perm}	partial pressure of gaseous species i on permeate side (Pa)
p_i^{ret}	partial pressure of gaseous species i on retentate side (Pa)
r	inner radius of a tubular membrane (m)
R	gas constant ($J\,mol^{-1}\,K^{-1}$)
T	temperature (K)

Greek symbols

δ	support thickness (m)
ε	porosity (–)
ξ_l	efficiency of channel l (–)
η	viscosity (Pa s)
λ	mean free path of molecules (m)
v_i	diffusion volume of gaseous species i (m^3)
τ	tortuosity (–)
$\partial\Omega_S$	symmetry boundary
$\partial\Omega_P$	boundary on the permeate side
$\partial\Omega_R$	boundary on the retentate side

References

[1] A.J. Burggraaf, L. Cot, Fundamentals of Inorganic Membrane Science and Technology, Elsevier, New York, 1996.
[2] S.L. Jorgensen, P.E.H. Nielsen, P. Lehrmann, Steam reforming of methane in a membrane reactor, Catal. Today 25 (1995) 303.
[3] N.E. Benes, A. Nijmeijer, H. Verweij, Microporous silica membranes, in: N. Kannellopoulos (Ed.), Recent Advances in Gas Separations by Microporous Membranes, Elsevier, Amsterdam, 2000.
[4] P. Dolecek, J. Cakl, Permeate flow in hexagonal 19-channel inorganic membrane under filtration and backflush operating modes, J. Membr. Sci. 149 (1998) 171.
[5] R.M. De Vos, H. Verweij, High-selectivity, high flux silica membranes, Science 279 (1998) 1710.
[6] R.D. Present, A.J. DeBethune, Separation of a gas mixture flowing through a long tube at low pressure, Phys. Rev. 75 (1948) 1050.
[7] E.A. Mason, A.P. Malinauskas, Gas Transport in Porous Media: The Dusty Gas Model, Elsevier, New York, 1983.
[8] E.N. Fuller, P.D. Schettler, J.C. Giddings, A new method for prediction of binary gas-phase diffusion coefficients, Ind. Eng. Chem. 58 (1966) 19.